Risk Analysis II, ed. C.A.Brebbia, Wit Press, 2000, vol.3, p.419-432.

Analysis of damage parameters of the Chi-Chi Taiwan earthquake

E. Lekkas
Department of Geology, University of Athens, Athens, Greece

Abstract

The Chi-Chi, Taiwan earthquake occurred on 21 September 1999 and caused extended casualties and property damage. Such an event is a manifestation of the active tectonic deformation in the region, which is the result of the convergence between the Eurasian and the Philippine tectonic plates. The geometrical and kinematic characteristics of the surficial expression of the seismic rupture are in good accordance with the instrumental recordings, which also show that the rupture was a composite one. This paper also addresses the geological site effects that contributed significantly to the damage distribution. The types of damage are presented, classified according to construction type, including large technical works. The causes of damage are then dealt with, together with an account of the spatial distribution of it, which is interpreted to be the result of the composite nature of the surficial fault break. It is also confirmed that a certain number of parameters were critical to the distribution and extent of damage.

1 Introduction

The Chi-Chi earthquake took place on 21 September 1999, at 1:47 am (local time). Its magnitude was M_w=7.5, the focal depth was 12 km and its epicentre was located at 23.82 N, 120.89 E. The main shock was followed by a dense aftershock sequence, which included three events with magnitude greater than 6.5 (M_w). The earthquake killed 2,465 people, injured 10,718, including about 1,000 people who were heavily injured. The regions affected most were the Taichung, Nantou and Taiching provinces, while the capital Taipei, which lies 150 km north of the epicentres, was less seriously affected. A total of 25,000 constructions were destroyed, 40,000 suffered considerable damage, and the number of people who lost their homes was around 200,000. The immediate cost

from infrastructure and building damage was estimated at US$ 10 billion, while the overall, long-term figure should be around US$ 30 billion.

In the following sections, we shall give an outline of the geodynamic and seismotectonic setting of the earthquake-hit area, together with the results of the instrumental recordings and the post-earthquake field reconnaissance. We then shall refer to the observed geological site effects, the type of construction damage and the distribution of the macroseismic intensities. All data will then be correlated and an attempt will be made to interpret the factors that affected the manifestation of damage, its typology and geographical distribution.

2 Geotectonic setting

Taiwan is located at a compressive tectonic boundary between the Eurasian Plate and the Philippine Sea Plate; the present convergence rate is about 7cm/year in a NW-SE direction. To the east of Taiwan, the Philippine Sea plate is subducting beneath the Ryukyu island arc, and to the south of Taiwan, the Philippine Sea plate is overriding the Eurasian plate along the Manila trench. Taiwan, therefore, occupies an unstable region between these two well-defined subduction systems of opposite polarity (Fig. 1).

From west to east the following major tectonic units can be distinguished (Chai [1], Chemenda [2], Suppe [3], Teng [4]) in Taiwan: (i) the Coastal Plain; (ii) the Western Foothills; (iii) the Hsuehshan and Backbone Ranges; (iv) the Tanano Basement Complex and (v) the Coastal Range. Units (i)-(iv) belong to the eastern margin of the Eurasian lithospheric plate, whereas (v) represents the leading, western edge of the Philippine Sea plate.

Specifically, the Coastal Plain consists of Pleistocene and younger terrace gravel, alluvium and well-bedded but poorly consolidated clastic sediments. Units (ii) and (iii) represent the active fold-and-thrust belt of western Taiwan. These Cenozoic strata represent continental shelf deposits, and are comprised of sandstone, quartzite, slate, argillite and tuff of Oligocene to Pliocene age. They are typified by imbricate thrusts and folds with west vengeance, reflecting up to 160-200 km horizontal shortening (Suppe [3]). The Backbone Range slate is a huge mass of dark gray phyllite intercalated with sandstone and limestone blocks of Eocene to Miocene age, and igneous rocks.

The Tanano Paleozoic – Mesozoic basement is composed of three lithologic units. The first has been interpreted as a Mesozoic mélange complex marking an ancient accretionary wedge or suture zone. The second consists exclusively of massive marbles dated radiometrically as Paleozoic. The third unit consists of metamorphosed Cretaceous granitoid rocks.

Eastward across the tectonic boundary along the Longitudinal Valley, which is a zone of modern intraorogenic left-lateral strike-slip vertical faults, lies the Coastal Range. It consists of Miocene arc calc-alkaline volcanics and associated sediments, forearc-basin flysch deposits, and the trench-basin Lichi mélange enclosing abundant olistostromal debris including the fragmented and dispersed East Taiwan Ophiolite.

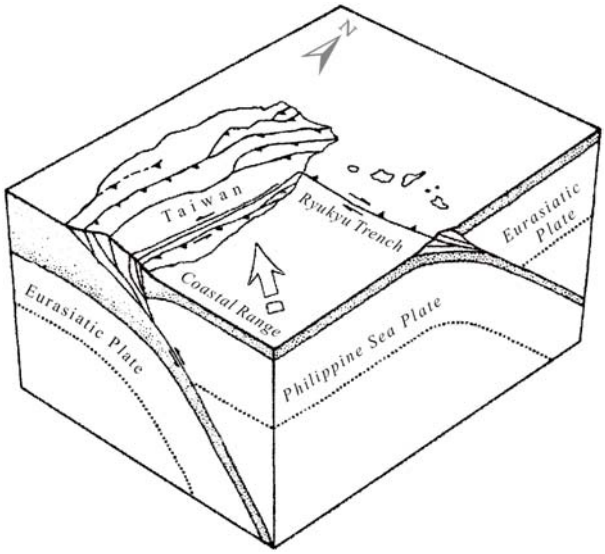

Figure 1: Schematic diagram showing present plate tectonic configuration of Taiwan.

Imbricated Neogene stratas in the Western Foothills were assembled as a combination of folds and thrust faults during the Pleistocene orogeny. The Tertiary strata consists of mainly unmetamorphosed sandstone and shale and have been flexed into NE-SW trending asymmetrical folds; at least seven major thrusts have been recognized.

The mechanism of thin-skinned tectonics has been used to explain the recognized fold-and-thrusting patterns in western Taiwan (Ho [5]). According to this model, thrusting was relatively shallow and confined to the cover sequence above the basement, resulting thin-skinned deformation. Related to these decollements, most thrust faults are east-dipping high-angle reverse faults.

Because of the oblique convergence and the indentation of the Philippine Sea plate, the fold-and-thrust belt of the majority of the Western Foothills developed a combination of contractional, transcurrent, rotational, and extensional deformation feautures, which resulted in thrusting, strike-slip and normal faulting (Suppe [6], Bonilla [7], Liu [8]). To the north, however, this fold-and-thrust belt is subjected to crustal stretching and rifting due to the flip of subduction of the Philippine Sea Plate (Teng [9]).

3 The seismic fault

A number of faults have been reactivated in Taiwan in the twentieth century (Fig. 2). However, their surficial traces were small, compared to that of the last earthquake (Bonilla [10]).

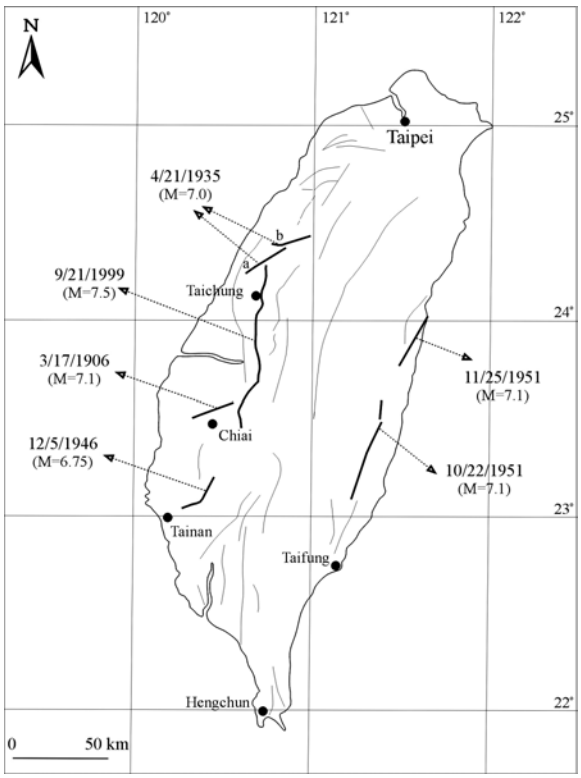

Figure 2: Faults that cut Quaternary formations and/or have been reactivated in earthquakes in the 20th century (modified from Bonilla [10]).

The Chi-Chi earthquake was caused by the rupture of the Chelungpu fault (Fig. 3). The main part of the fault is a north-south-striking thrust fault that dips about 30 degrees to the east. It is part of the western thrust zone that accommodates some of the crustal shortening caused by the collision of the Philippine Sea Plate and the Eurasia Plate. At the north end of the rupture, there is a sharp bend to the east and the fault rupture strikes nearly east-west. The total length of the rupture is about 80 km, with a down-dip width of about 40 km. The epicenter is located about 15 km from the south end of the fault. This earthquake had a very energetic aftershock sequence with M_w>6.5 shocks in the first week.

The rupture resulted in fault scarps 2 to 4 m along the southern end of the rupture and 4-9 m high in the northern end, but some of the largest scarp heights include the effects of folding in the hanging wall. At the northern end, the complex east-west-striking rupture consists of multiple strands, including normal faulting steeply dipping to the north. The hypocenter at Chi-Chi lies very close to the Shungtung fault and occurred at depth 12 km near the intersection with the Chelungpu fault (Fig. 4).

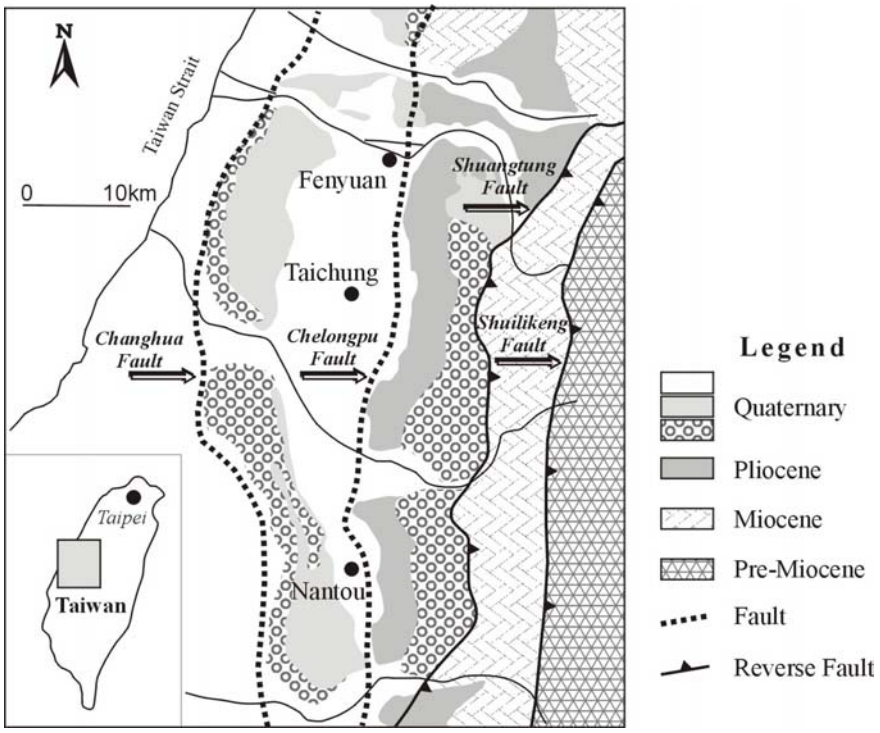

Figure 3: Schematic map showing the traces and general geology of the 9-21-99 earthquake region (after Ho [5] with modifications and additions).

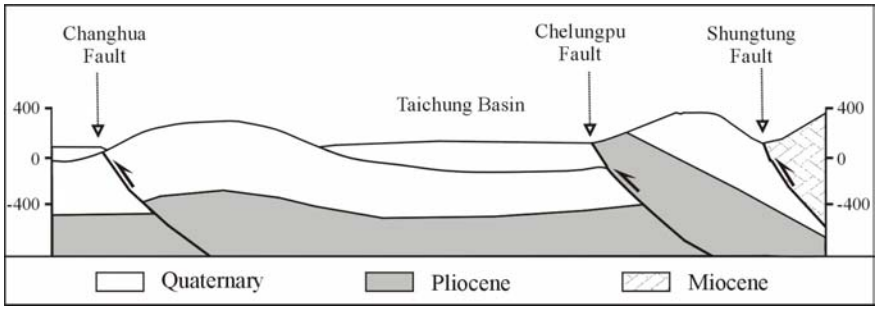

Figure 4: Schematic E-W cross-section, to show the neotectonic deformation and the location of the seismogenic Chelungpu fault.

As we shall see in the following paragraphs, the fault trace ran through both small buildings and large, important technical works, as the Tachia River Dam, near the town of Shih-Kang; at this location, the fault had not been mapped (Ho

[5]). Moreover, the seismic fault trace deviated at numerous locations from the mapped geological fault, which means that fresh fracture surfaces were created in the Chi-Chi earthquake, signifying a complex fault zone.

4 Instrumental data

According to the existing data, the magnitude of the shock was M_w=7.5; its epicentre was located at 23.82 N, 120.89E. The focal depth was h=12 km and the fault plane solution gave a reverse, NE-SW-trending fault (strike, dip, slip = 026, 27, 82) (TCWB [11]). It should also be noted that the solutions provided by the seismological centres worldwide (Harvard, USGS, etc) were somewhat different from each other. The location of the epicentre is east of the surficial traces of the Chelongpu and Shuangtung faults, but the focus is correlated to the rupture surface of the former, which had the most extensive surficial expression.

According to the data evaluation and processing, the rupture surface extends 50 km north and 30 km south of the initial rupture point, which shows that the rupture propagation was mostly unilateral (Fig. 5). The initial direction of rupture was towards the SW, then towards the NE and then again towards the SW. The maximum calculated focal displacement was 6 m and the average was 2.5 m, on an 80km × 30km rupture surface (Yagi [12]).

About 400 portable accelerometers were spread throughout the greater area, while there was several others located at large technical works (bridges, dams, etc.), a fact quite helpful for the interpretation of the damage pattern. As shown on the preliminary shake map of figure 6, there is a clear correlation between the acceleration pattern and the surficial seismic fault trace. While the peak accelerations were maximum at the southern termination of the rupture, the peak velocities reached their maximum values at the northern tip of the fault; at that location, the largest fault slip and displacement were observed. In addition, a rapid westward attenuation of the acceleration is obvious, while the opposite holds for the eastward direction (Fig. 7).

One station located near the bend in the rupture, recorded a ground motion with peak velocity of about 300 cm/s, which is the largest peak velocity ever calculated. The time history and response spectra for this station are shown in figure 8. The horizontal peak ground accelerations (PGA) from the Chi-Chi earthquake were larger than median PGAs predicted by the attenuation relations used to develop Taiwan's building code.

5 Geological site effects

The following earthquake-induced site effects were related to the 21 September earthquake, within the meizoseismal area:

Landslides. Landslides and rock-falls destroyed the highway transportation systems and isolated the communities in the central mountain areas of Taiwan. There where two enormous landslides at Tsaoling and Nankang, 30 km south and 13 km north of the Chi-Chi epicenter, respectively. The debris flow of the Tsaoling landslide traveled a distance of 2-3 km, carrying with it buildings, roads

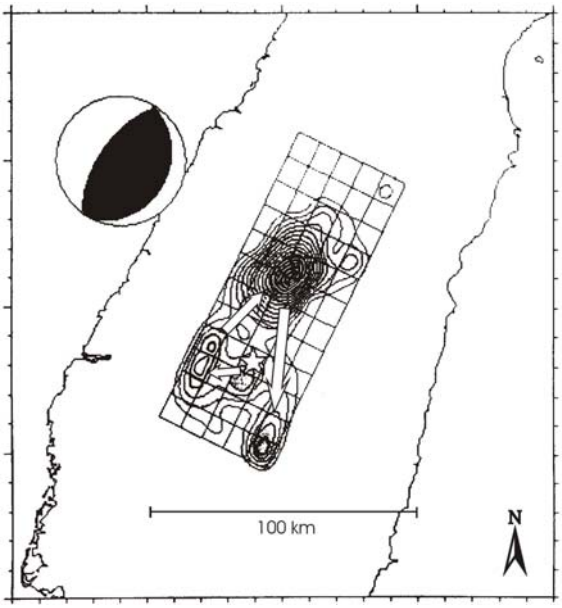

Figure 5: Rise time plot along the seismic surface (TCWB [11], Yagi [12]).

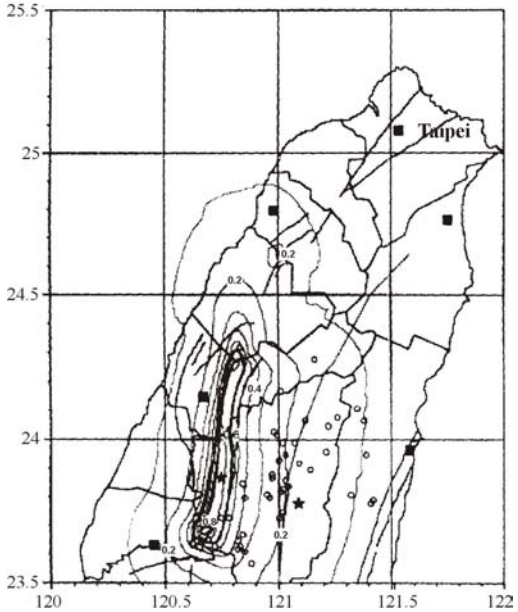

Figure 6: Preliminary shake map (TCWB [11]).

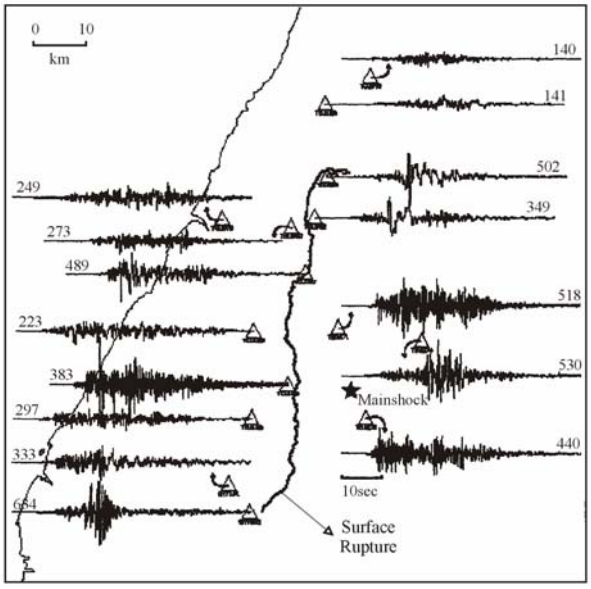

Figure 7: East-west component of some samples of near-source strong-motion acceleration records. The number above the waveform trace is the peak acceleration value (PGA) in cm/sec/sec (TCWB [11]).

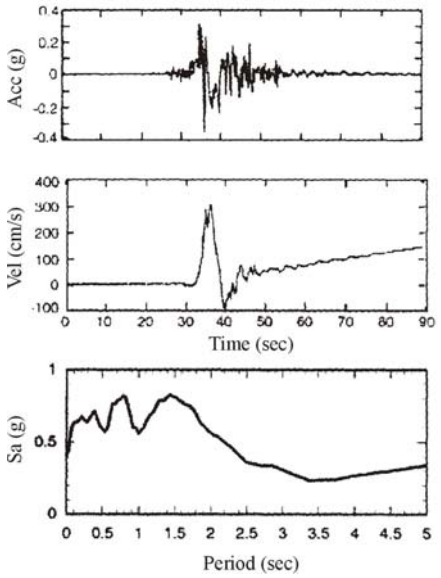

Figure 8: Time history and response spectra (TCWB [11]).

and cars. About forty persons were killed. The debris flow of the Tsaoling landslide dammed the valley and formed an artificial lake.

Liquefaction. Liquefaction occurred at a number of sites, causing considerable damage. It was significant at Yuan-lin- there was widespread settlement of building foundations, and water wells were completely filled by sand from sand boils. Liquefaction also led to settlement, failure and lateral spread of levees, and movements at bridge abutments at river crossings. However, despite signs of liquefaction and lateral spread close to the bridge foundations. Thaichung port, located some 45 km from the epicenter, experienced liquefaction-induced damage at the quays, port facilities and storage locations. More than twenty sites in the meizoseismal area were also affected by liquefaction, which damaged the road network, infrastructure and other facilities (Fig. 9).

Soil fractures. The main shock caused a multitude of soil fractures, mostly within unconsolidated surficial deposits. Those fractures were mainly shallow, but at cases their length exceeded 500 m.

6 Earthquake damage

As mentioned above, the earthquake caused extensive damage to the urban environment. The damage extends roughly along the fault trace and stretches beyond its northern and southern ends. Pockets of heavy damage were located all over the greater area and mainly to the north, in the neighborhood of Taiwan and to the south, but also along the west coastal area.

Damage was more severe at sites located on the hanging-wall block, which seems to have received the largest amount of seismic energy. Along the fault trace and on the hanging wall side, a «compression» zone, about 100 m wide was observed. Within this zone most buildings collapsed or suffered heavy structural damage; on the other hand, damage was relatively low on the footwall side. This is in accordance with instrumental data (Fig. 7), which show that the values of the recordings of the free-field accelerometers are considerably higher. The whole picture contrasts with the one obtained from the Kobe (Japan) and Izmit (Turkey) earthquakes (Lekkas [13]), where the predominant fault motion was strike-slip. In addition, despite the fact that displacement was larger at the northern portion of the fault, the damage at that area was relatively lower. This is reflected in the distribution of accelerations, which shows larger values of peak accelerations at the southern portion, a direct consequence of the rupture mechanism.

The damage for every construction type can be described as follows:

Single-Story Houses. In rural areas, traditional one-story, 30-80 - year-old residences are constructed of unreinforced masonry or adobe with weak mortar and with wood roofs. In areas of intense ground shaking, these buildings performed poorly and caused a number of deaths.

Arcade Buildings. They are very common in Taiwan, and many of them were damaged. These buildings have open fronts at the street with covered pedestrian walkways created by the second-story framing. Usually, the street

level is commercial or parking and the upper stories are residential; this style creates an undesirable soft story at the lowest level. Three- and four-story arcade buildings are common, bur in the more densely populated areas, heights up to 12 are not unusual.

Mid-Rise Buildings. In urban areas, a substantial percentage of the residential units are in reinforced apartments of 12-15 stories. A number of these buildings collapsed in special Taichung City, Feng-Yuan, Dali and Taipei County. Typically, they are cast-in-place, special moment frame structures utilizing all frame lines in both directions. They generally have spread footings (Fig. 10). The exterior walls and the shaft walls are reinforced concrete, approximately 10 cm thick. These are considered nonstructural walls and are not included in the seismic design (EERI [14]).

High-Rise Buildings. Καταρρεύσεις και severe damage to hifh-rise buildings (20 stories or more), but there were reports and observations of minor damage to facades and some movement at the construction joints at floors. Many of Taiwan's recent high-rise buildings (generally over 25 stories) are constructed with structural steel.

Dams. Fault rupture beneath the Shih-Kang Dam (45 km from the epicenter) caused severe damage and cut off the water supply from the reservoir. Fault rupture through a water treatment plant in Feng-Yuen rendered the plant inoperable. In addition, the earthquake resulted in a large number of leaks or breaks in the transmission and distribution network. Damage to Shih-Kang dam reduced the water supply for Taichung City and County by between 40% and 50%.

The Feng-Yuen water treatment plant consists of settling basins, finish water reservoirs and associated underground piping, all of which were damaged. A number of pools in one settling basin used baffles in the treatment process. The submerged baffles were displaced due to sloshing. The sloshing was so severe that some baffles actually flipped out of their individual polls and ended up on the ground outside the settling basin. Portions of the reinforced concrete roofs over the finished water reservoirs collapsed. The fault rupture passed directly through one corner of the plant. The vertical offset at the fault trace was about 5 m, and the horizontal offset was in the 1 to 2 m range.

Bridges. Some bridges failed due to fault rupture beneath or adjacent to them. Rupture through a bridge was identified in three cases; rupture immediately adjacent was identified as a cause of a fourth collapse, and rupture was suspected in connection with the collapse of a fifth bridge. Given the magnitude of fault offsets, significant damage and collapse were not surprising.

The U-Shi Bridge, located about 18 km NW of the epicenter, consisted of two parallel structures –the East Bridge constructed in 1981 and the West Bridge constructed in 1983. The superstructure comprised 18 spans of prestressed I-griders supported on reinforced concrete pier walls. The deck had an expansion joint at the north abutment, continuous joints for the next two piers, and another expansion joint over the third pier. Fault rupture passed through the foundation of the third pier with an offset of approximately 1.5 m vertical.

Figure 9: Partial view of the affected area. The port facilities (arrow), which were damaged by liquefaction, are visible.

Figure 10: Representative types of collapsed mid-rise buildings.

The fault ruptured beneath the I-Jiang Bridge about 25 km NW of the epicenter. This structure comprised 24 spans simply supported without bearings on reinforced concrete pier walls. When the rupture passed between the first and second piers from the northwest abutment, the first pier rose approximately 3 m relatively to the second pier. In its final rest position, the deck overhangs the pier wall by approximately 4 m.
All four spans collapsed in the Toong-Tour Bridge, near the southern end of the fault rupture about 25 km SW of the epicenter.
The Jyi-Luh cable-stayed bridge across the Choshun River, about 10 km SW of the epicenter, was under construction and sustained significant damage. The bridge deck had not been completed near the pylon. The soil around the supporting bents had apparently liquefied, and may have permitted some to settle and rotate. The shear keys at both ends of the stayed spans apparently had translated laterally approximately two meters, gouging the supporting bent cap and inducing severe shear cracking. The pylon spalled to expose the core concrete and reinforcement over approximately two meters in height; splitting of the concrete around the core was evident nearly to the height of the lowest cables.

Electric Power System. In Taipei (150 km from the epicenter), the power went out even before the city began to shake because the shock initiated the power cut-off system. Although the power generation facilities remained largely operational, there was substantial damage to substations and high-voltage transmission towers. Many hgh-voltage transmission towers were damaged; some collapsed, while others tilted or settled due to ground deformation. The Chung-Liao substation, less than 10 km from the epicenter, was severely damaged by a combination of strong shaking and permanent ground deformation effects.

Industrial units. The shock hit a large number of industrial facilities, located all over the epicentral area. The units located on the fault trace were totally destroyed and those that lay away from the fault suffered significant damage, too. In many cases the damage was due to liquefaction, lateral spreading, etc. Damage to some of the industrial units is also attributed to their structural characteristics, as large open spaces, structural asymmetry, etc.

7 Discussion-Conclusions

The earthquake M_w=7,5 that hit Taiwan on 21st September and the dense aftershock sequence are attributed to the intense geodynamic processes of the area due to the composite nature of the collision of the Philippine Sea and the Eurasian Plates. This procedure resulted in the development of characteristic neotectonic features, which are typified by folds and reverse faults striking N-S in West Taiwan. Instrumental and field data allow us to draw the following conclusions:

- The earthquake was caused by the rupture on the Chelungpu reverse fault which was accompanied by a parallel composite reverse fault surface with a maximum offset of about 9 meters and general NE-SW strike, whose

geometry and kinematics vary at different places. The geometrical and kinematic characteristics of the fault coincide with the geotectonic setting of the area and consequently with the neotectonic processes.

- The seismic rupture did not completely coincide to the mapped Chelongpu fault, and the deviation was up to hundreds of meters at many places. This is ascribed to the composite nature of the seismogenic area and the huge tectonic stresses, and therefore the deformation was accommodated by more than one fault surfaces.
- Despite this fact, the characteristics of the seismic fault are in good accordance with the instrumental data. The observed deviations are justified by the differentiation of the geological conditions between the source area and the affected sites, the accuracy of the instrumental recordings, and so on. It is important to mention that the earthquake source was located at the south of the seismic rupture, while the maximum fault offset was observed on the northern part, gradually decreasing southwards.
- The damage was generally accumulated along the main fault trace but also stretched beyond its northern and southern ends. Damage pockets were mainly located along the western coastal area, where the geological earthquake-induced site effects played a significant part.
- Almost all constructions that lay on the fault trace collapsed or suffered heavy structural damage.
- The general damage conditions on the hanging wall were justified by the instrumental data, according to which the acceleration values were higher on the eastern block than on the western.
- The heaviest damage occurred on the hanging wall along a 100-m wide zone, which seems to have received the largest amount of seismic energy and consequently was subjected to intense deformation. This picture contradicts observations from other earthquakes (Turkey-Izmit, 17 August 1999) where the horizontal, not the dip-slip component was predominant (Lekkas [13]).
- Buildings up to 15 stories (50 m total height) suffered the most seismic damage, including collapses. However, compared to the total stock of such buildings, and considering the magnitude of the earthquake, the percentage of damage was small. The damage to these buildings could be attributed to the soft first story created by the «open space» policy, or to poor construction.
- High-rise buildings (more than 50m height) did not collapse and suffered only non-structural damage.
- Many buildings that collapsed or suffered severe damage had been subjected to important alterations, such as the removal of many internal walls during remodeling.
- Liquefaction and landslides are responsible for considerable damage that occurred on buildings and mainly on infrastructure works, as dams, bridges, etc. Such site effects contributed locally to the failure of these constructions.
- The surficial fault break mechanism did not produce unilateral rupture directivity effects from the seismic source to a site but a complicated bilateral propagation pattern. This propagation the inhabited areas located at the SW and NE prolongation of the fault trace, including the capital Taipei.

After the qualitative description of the above parameters, there will be an attempt to quantify them in the near future through refined analysis of instrumental data and the post-earthquake field reconnaissance and site tests. Such a procedure may contribute to the reduction of the consequences in significant seismic events.

References

[1] Chai, B.H.T. (1972). Structure and tectonic evolution of Taiwan. *American Journal of Science*, 272, 389-422.

[2] Chemenda, A.I., Yang, R.K., Hsieh, C.H. & Groholsky, A.L. (1997). Evolutionary model for the Taiwan collision based on physical modeling. *Tectonophysics*, 274, 253-274.

[3] Suppe, J. (1981). Mechanics of mountain building and metamorphism in Taiwan. *Memoir Geol. Soc. China*, 4, 67-89.

[4] Teng, L.S. (1990). Geotectonic evolution of late Cenozoic arc-continent collision in Taiwan. *Tectonophysics*, 183, 67-76.

[5] Ho, C.S. (1986). An introduction to the geology of Taiwan: Explanatory text of the Geologic Map of Taiwan. Central Geological Survey, Taipei, Taiwan, RO China, 192pp.

[6] Suppe, J. (1986). Reactivated normal faults in the western Taiwan fold-and-thrust belt. *Memoir Geol. Soc. China*, No 7, 187-220.

[7] Bonilla, M.G. (1977). Summary of Quaternary faulting and elevation changes in Taiwan. *Memoir Geol. Soc. China*, No 2, p. 43-55.

[8] Liu, C.Y., Yu, S.B. & C.H.T. (1998). Neotectonics of the Taiwan Mountain Belt. In Flower et al. (eds) Mantle Dynamics and Plate Interactions in East Asia. American Geophysical Union, Geodynamic series, V. 27, p. 301-315.

[9] Teng, L.S. (1996). Extensional collapse of the northern Taiwan mountain belt. *Geology*, V. 24, p. 949-952.

[10] Bonilla, M.G. (1975). A review of recently active faults in Taiwan: U.S. Geological Survey Open File Report 75-41, 58p.

[11] Taiwan Central Weather Bureau (1999). Preliminary Shake Map of Taiwan earthquake. http://www.cwb.gov.tw.

[12] Yagi & Kikuchi (1999). Spatiotempoal distribution of source rupture process for Taiwan eathquake (M_s=7.7). http://wwweic.eri.u-tokyo.ac.jp/yuji/Taiwan/Taiwan.html.

[13] Lekkas, E., Dandoulaki, M., Ioannides, K., Lalechos, Σ. & Kiriazis, A. (1999). Izmit earthquake, Turkey 1999. Seismotectonic settings – Earthquake and Ground motion characteristics – Geodynamic phenomena – Geographical distribution & damage typology. 13th Hellenic Concrete Conference, Special Issue, Rethimno.

[14] EERI (1999). The Chi-Chi, Taiwan Earthquake of September 21, 1999. *Special Earthquake Report*, December 1999.